MICROSCOPY RESEARCH AND TECHNIQUE 42:433–450 (1998)

Sympathetic Neuromuscular Transmission at a Varicosity in a Syncytium

M.R. BENNETT,* A. CHEUNG, AND K.L. BRAIN
The Neurobiology Laboratory, Department of Physiology, Institute for Biomedical Research, University of Sydney, NSW 2006 Australia

KEY WORDS junction; synapse; smooth muscle; syncytium

ABSTRACT The autonomic neuromuscular junction at a varicosity in the vas deferens is defined by the localization of the vesicle-associated protein syntaxin in high concentrations in the axolemma and a high density of $P2x_1$ receptors in a cluster beneath the varicosity. Calcium fluxes have been observed in all individual varicosities of a nerve terminal on the arrival of an impulse even though recordings made from these varicosities of the electrical signs of transmission with loose-patch electrodes over the varicosities show that they have very different probabilities for the secretion of a quantum. The fact that some varicosities seldom release a quantum on the arrival of an impulse is supported by the observation that antibodies against the N-terminus of synaptotagmin, which uniquely label the inside of synaptic vesicles when they undergo exocytosis, fail to do so in some varicosities during nerve stimulation whereas they do in others. It is suggested that the probability for secretion from a varicosity depends on the number of secretosomes that the varicosity possesses, where a secretosome is a complex of syntaxin, synaptotagmin, an N-type calcium channel, and a synaptic vesicle. *Microsc. Res. Tech. 42:433–450, 1998.*

INTRODUCTION

This is the one hundredth anniversary of the naming of the autonomic nervous system by Langley (1898). His laboratory went on to develop the idea of chemical transmission (Elliott, 1904; Langley, 1901) as well as that of the transmitter receptors on effector cells (Langley, 1906). The development of these concepts was dependent on investigations that Langley and his colleagues made on transmission at sympathetic and somatic nerve endings. In the first half of this century, the paradigm synapse for understanding transmission was that provided by autonomic neuromuscular junctions, especially in the hands of Dale, Loewi, and their colleagues (Dale, 1934). In the latter half of this century, studies of the somatic neuromuscular junction came to dominate our thinking on the mechanism of transmission at synapses, principally because of the relative accessibility of this junction to the newly invented biophysical techniques, such as the microelectrode. Indeed, it is just 50 years since Katz first detected miniature endplate potentials in 1948 (Katz, 1996), an observation that led directly to the concept of a quantum of transmitter action (del Castillo and Katz, 1954). This observation more than any other placed the somatic neuromuscular junction at centre stage in the elucidation of mechanisms of synaptic transmission. It may well be asked as to why the sympathetic neuromuscular junction failed to retain its dominant position in the study of synapses. There are three principal reasons for this. The first relates to the relatively simple geometry and accessibility of the somatic junction for electrophysiological analysis compared with that of sympathetic nerve terminals (Bennett, 1996b). The second concerns the fact that smooth muscle cells and cardiac muscle cells are coupled in an electrical syncytium making the interpretation of electrical signals that occur during transmission more complex than that at the somatic junction, for which the cable equation has seemed adequate to interpret such electrical signals (Fatt and Katz, 1951; see however, Thomson et al., 1995). Finally, there is the difficulty that whilst the principal transmitter at the somatic junction was early recognized and the receptor distribution for acetylcholine ascertained due to the use of alpha bungarotoxin (Katz and Miledi, 1973), this has not been the case for the sympathetic junction, for which agreement has only recently been reached as to the principal transmitters involved, so that the distribution of receptors for these transmitters is only now being realized.

In this short review, consideration is given to very recent technical developments and discoveries that have radically changed our capacity to probe the workings of the sympathetic neuromuscular junction (for a consideration of earlier observations, see Bennett, 1996a). These include the use of antibodies against vesicle-associated proteins to delineate the sites of release of transmitter on varicosities and so help define the junction (Brain et al., 1997). A bidomain analysis for determining the current flow that occurs in a syncytium following the release of a packet of transmitter has been developed (Henery et al., 1997) and loose-patch recording techniques utilized for recording these currents around a single transmitting varicosity (Macleod et al., 1994). Antibodies have been developed against both intracellular and extracellular domains of the purinergic P2x receptor class that now allow for the spatial distribution of these ionotropic receptors to be deter-

*Correspondence to: M.R. Bennett, The Neurobiology Laboratory, Department of Physiology, Institute for Biomedical Research, University of Sydney, NSW 2006, Australia. E-mail: maxb@physiol.usyd.edu.au

Received 23 March 1998; accepted in revised form 10 May 1998

mined with respect to varicosities that use ATP as a principal transmitter (Hansen et al., 1997). Finally, calcium indicators have been coupled to dextran in order to introduce them into sympathetic nerve terminals for the purpose of ascertaining the calcium changes that occur in single varicosities following a nerve impulse (Brain and Bennett, 1997). Sympathetic nerves to the smooth muscle of the vas deferens are the preparation of choice in these studies, which attempt to provide a new level of clarity for what constitutes autonomic neuromuscular transmission. It may now be argued that the junction formed by varicosities with smooth muscle cells in this organ provides a more appropriate paradigm for the understanding of central synaptic transmission than does any other junction of the peripheral nervous system.

STRUCTURE OF THE SYMPATHETIC NEUROMUSCULAR JUNCTION

In his pioneering studies Hillarp (1946) showed unequivicolly that the innervation of smooth muscles is by varicose nerve terminals. However, it was not until the advent of the electronmicroscope that Richardson (1962) and Merrillees (1968) were able to provide us with a comprehensive view of the relationship between these varicose endings and smooth muscle. These studies are summarized in the diagram of Figure 1. This shows that there are small bundles of three to seven varicose axons, partially or wholly enveloped in Schwann-cell sheath, both on the surface of the muscle as well as in the body of the smooth muscle bundles that comprise the organ. In addition, single varicose axons can be found on the surface and in the muscle bundles that become divested of Schwann cell in the region of apposition between the varicosities and smooth muscle cells. Many smooth muscle cells in a transverse section through a muscle bundle show regions of very close apposition to adjacent cells at which connexins form junctions between the cells (Fig. 1), providing for electrical continuity between the cell interiors. Unlike in cardiac muscle, where the junctions formed by connexins are confined to the ends of the cardiac myocytes, smooth muscle junctions formed by the connexins occur along the length of the muscle cells as well as towards their ends.

Recently the distribution of varicosities in the vas deferens has been studied using the method of loading the cut ends of the sympathetic axons with dextran-rhodamine. This complex is then transported into the endings so that fluorescent axons can be identified with confocal microscopy at high resolution throughout muscle bundles of intact vas deferens. Figure 2 shows single varicose axons labelled in this way in the longitudinal muscle. The distance between the varicosities, which are readily distinguished by the sudden increase in volume of the fluorescent profile, is between 4 and 7 μm. These varicosities, occurring together on a string, have a length of about 1.6 μm and a width of 0.6 μm (Fig. 3A and B) giving a width to length ratio of 0.38 (Fig. 3C).

The arrows point to varicosities that occur at branch points of the sympathetic axons, referred to as nodal varicosities. These are generally wider than those on a string (1.2 μm compared with 0.6 μm) but have about the same length (see Fig. 3A and B). When two strings of varicosities originate at a node, the individual varicosities of each string frequently are aligned, as shown in Figure 2B, so that without confocal microscopy they might be taken as constituting a single string, especially given that they can be apposed for distances of less than 1 μm (Fig. 2B).

The characteristics of varicosity strings observed with rhodamine fluorescence can be compared with that arrived at by analysis of serial transverse sections through the sympathetic nerves in the vas deferens after examination with the electronmicroscope. These serial section studies with the electronmicroscope are summarized in the diagram of Figure 4: the varicosities are about 1.1 μm long and 0.5 μm wide, separated from each other by distances of about 5 μm (Cottee et al., 1996), results similar to those obtained using rhodamine fluorescence. This electron microscope shows that synaptic vesicles tend to be clustered towards the region of close apposition with the muscle cells, although they are generally found occupying a volume of the varicosity that amounts to 80%. The distribution of synaptic vesicles within a varicosity can also be determined using fluorescent labelled antibodies against the ubiquitous synaptic vesicle associated proteoglycan SV2 in conjunction with the dextran-rhodamine labelling of the varicosity. Figure 5A(a) shows three varicosities filled with dextran-rhodamine and Figure 5A(b) the distribution of SV2 in the same three varicosities. The vesicles are clustered into a discrete mass that occupies a volume about 80% of that of the entire varicosity with which they belong, in agreement with the electron microscope observations.

Electron microscopy of serial sections through varicosities of single axons that become partially devoid of Schwann cell sheath shows that they come into close apposition with smooth muscle cells of about 50 nm over a very small area of less than 0.06 μm^2; for regions of apposition of less than 100 nm this area is about 0.2 μm^2 (Cottee et al., 1996). This is the case whether the varicosities are at the surface of the muscle or in the muscle bundles. In the case of varicosities in axon bundles within the muscle, those that become partially devoid of Schwann cell sheath only come into appositions of about 150 nm over an area of about 0.2 μm^2. The question arises as to the site at which synaptic vesicles may undergo exocytosis from the varicosity membrane, that is identification of the extent of the active zone of the varicosity: is this confined to a region of apposition to the smooth muscle cells of 50 nm as is often claimed? At the somatic neuromuscular junction, the active zones are found spaced about 1.5 μm apart, and these occur at regions of relatively high concentration of the vesicle-associated protein syntaxin, which anchors the synaptic vesicle to the plasmalemma in the process of exocytosis (Boudier et al., 1996). The distribution of high concentrations of fluorescent syntaxin antibodies in sympathetic varicosities is shown in Figure 5B(b) in relation to the accumulation of synaptic vesicles in the varicosities labelled with SV2 shown in Figure 5B(a) (Brain et al., 1997): syntaxin occupies a relatively smaller area in the photomicrograph compared with

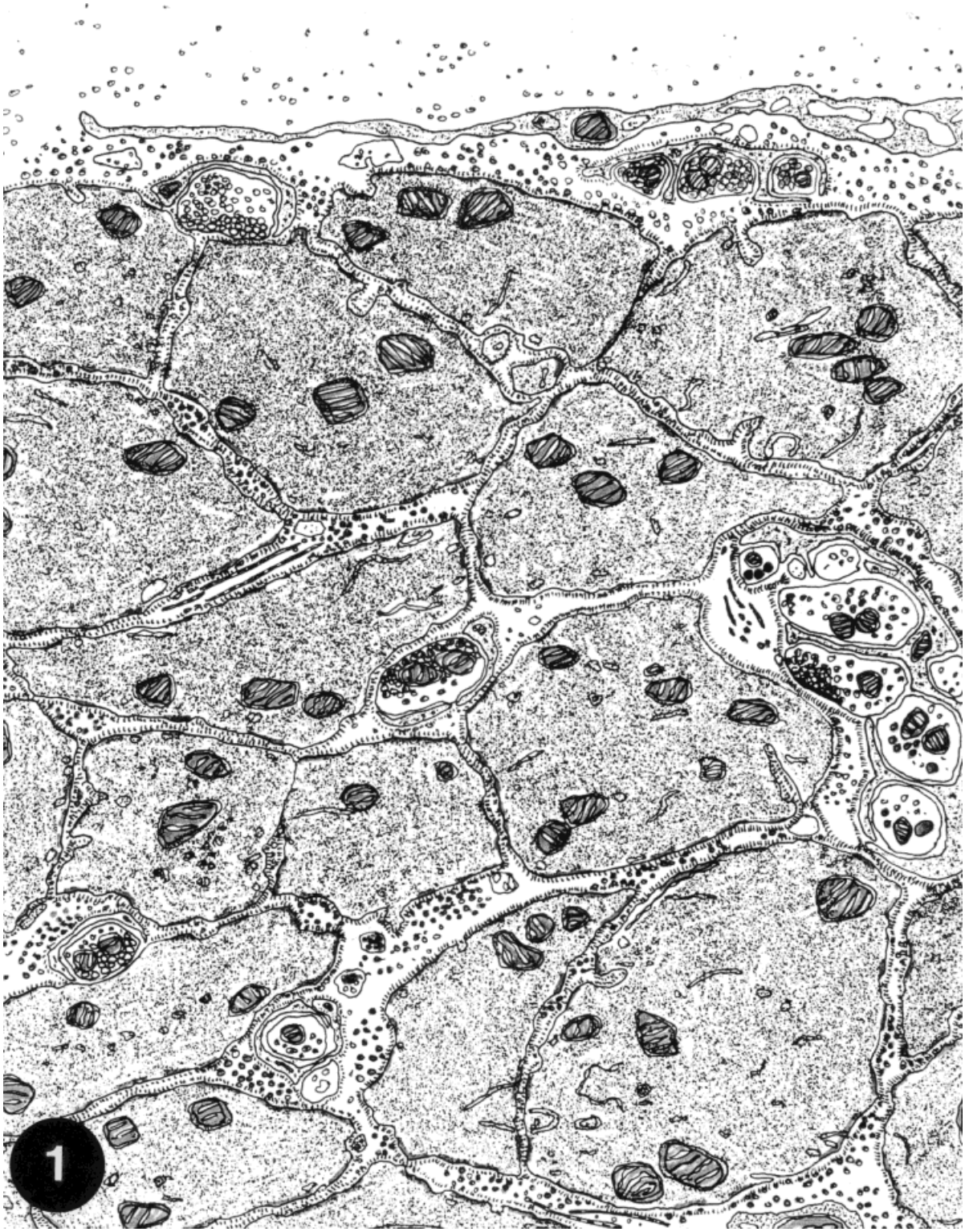

Fig. 1. Diagram of the structure of a visceral smooth muscle at the ultrastructural level. This drawing is of a transverse section through the longitudinal muscle of the guinea-pig vas deferens. Individual smooth muscle cells are electrically coupled at sites of very close apposition between their membranes where connexions are found. Most of the nerves at the serosal surface are in axon bundles although occasionally single axons partly bare of Schwann cell can be found in close apposition with smooth muscle cells. In the deeper layers of the muscle, both axon bundles and many individual varicose axons can be observed, some of which come into such close apposition with the muscle that basement membrane is excluded (diagram by G. Bennett, unpublished observations).

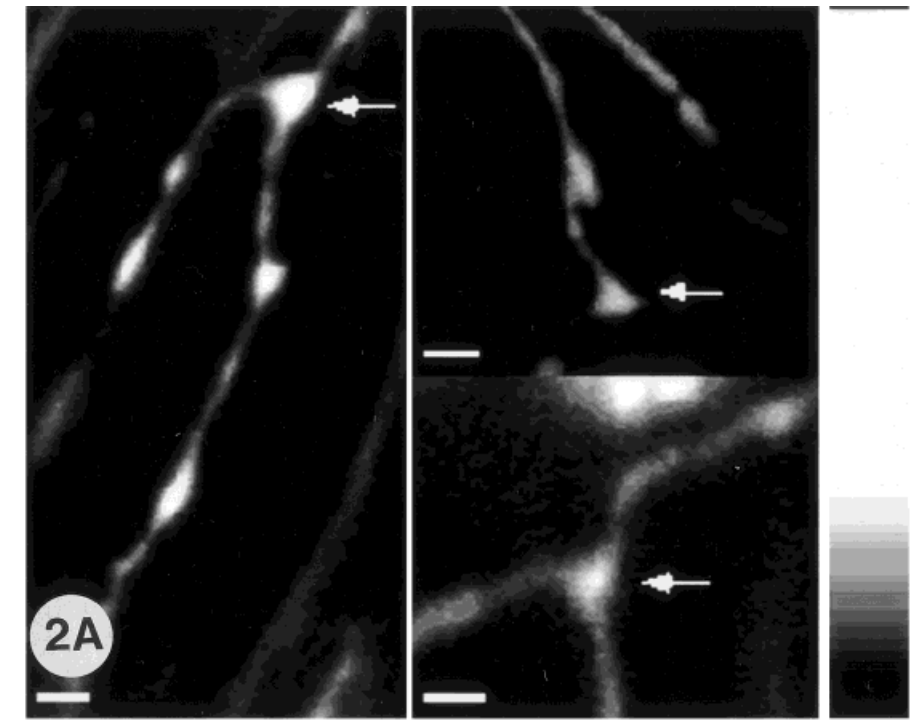

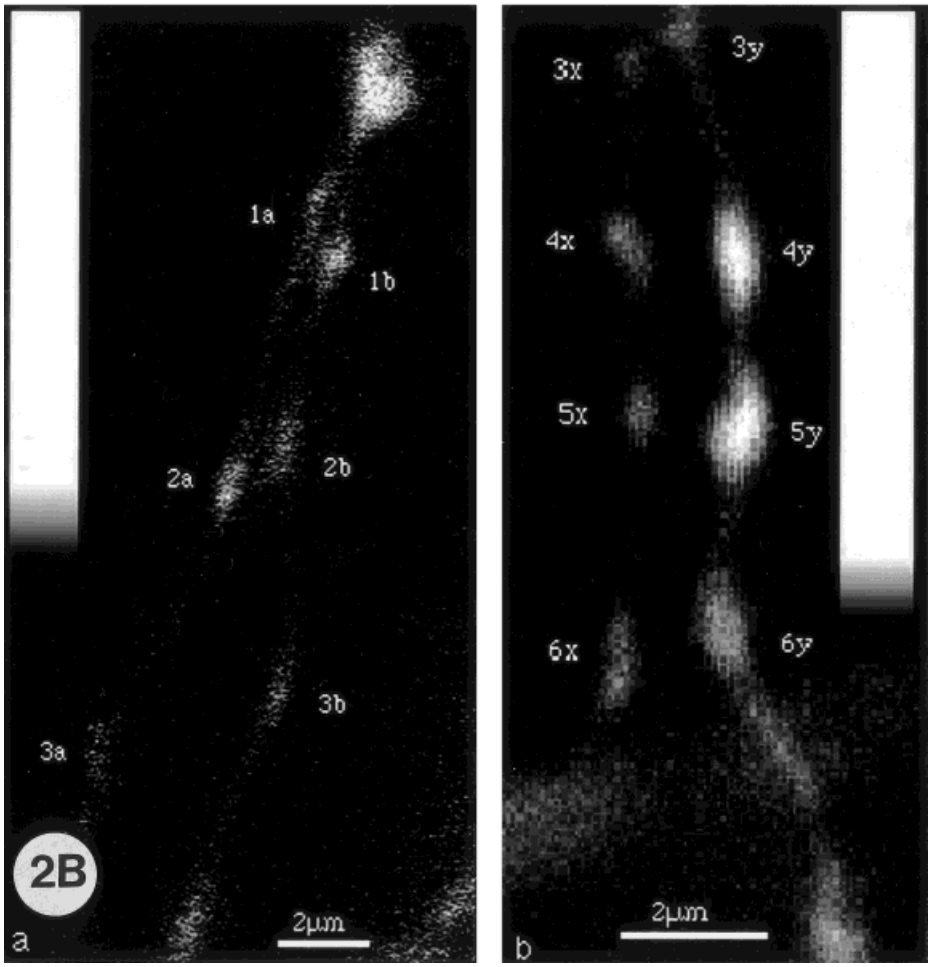

Fig. 2. **A:** Nodal varicosities. Oregon Green 488 BAPTA-1 fluorescence images of nodal varicosities (arrows) from three different experiments are shown. False colour scale is to the right. Scale bars = 2 µm. **B:** (a) Oregon Green 488 BAPTA-1 fluorescence of two strings of varicosities are shown; varicosities 1a and 1b, as well as 2a and 2b are approximately 1 µm apart, while 3a and 3b are separated by approximately 5 µm. (b) Two strings of varicosities from a different experiment to (a) are shown. The varicosity pairs 3x and 3y, 4x and 4y, 5x and 5y, as well as 6x and 6y are all between 1 and 2 µm apart. Varicosity separation was arbitrarily defined as the distance between the centres of fluorescence of each varicosity in a specified pair. Corresponding look up tables (LUT) and scale bars (2 µm) are shown. All varicosities shown responded to electrical stimulation from Cheung and Bennett (unpublished observations).

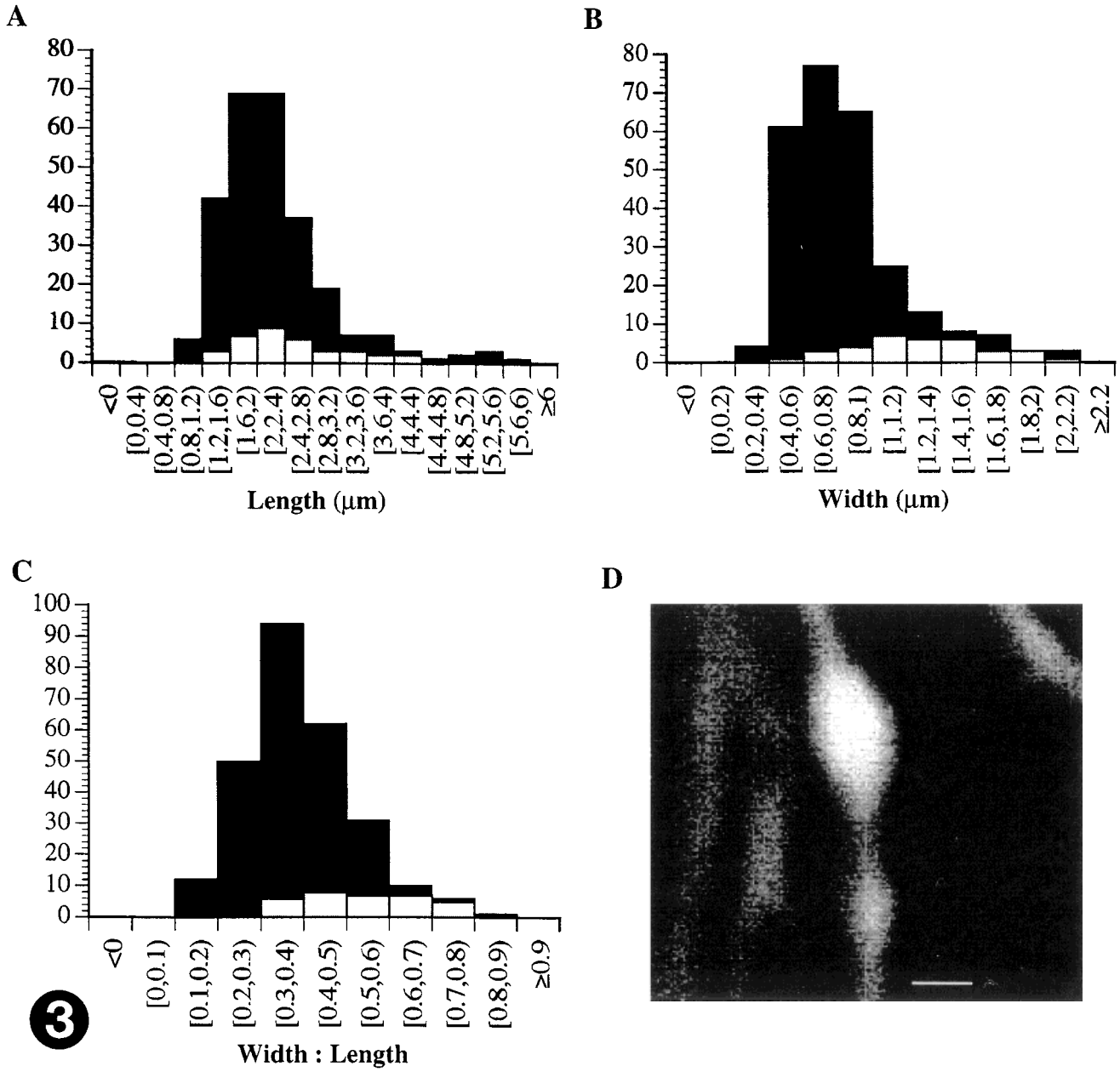

Fig. 3. Varicosity dimensions. The size-frequency histograms of nodal varicosities (gray histograms) are shown superimposed on that of non-nodal varicosities (black histograms). **A:** Frequency histogram of varicosity lengths. **B:** Frequency histogram of varicosity widths. **C:** Frequency histogram of width: length ratios. **D:** Oregon Green 488 BAPTA-1 fluorescence image of two adjacent varicosities showing very different dimensions. Calibration bar = 2 μm. From Cheung and Bennett (unpublished observations).

that of SV2, which occupies an area of about 0.25 μm^2 of plasmalemma. Given that syntaxin is occurring at the region of closest apposition of the varicosities to the smooth muscle cells, then according to the electron microscope results given above, an area of close apposition of about 0.25 μm^2 occurs for distances up to about 100 nm. This calculation then suggests that the active zone region occurs over distances of the varicosity membrane from the smooth muscle cells of about 100 nm. As the distance of close apposition over this area of 0.25 μm^2 varies from less than 50 nm to just over 100 nm, the diffusion distance for a vesicular release of transmitter to the smooth muscle also varies over at least 50 to 100 nm. Monte Carlo simulations have shown that the release of ATP onto a receptor patch over distances that vary by this amount will give rise to at least a twofold difference in the rise time and amplitude of the junctional current (see table 1 in Bennett et al., 1995). It would be expected then that considerable variation might occur in the amplitude and time course of junctional currents generated by the same size quantum of ATP released at the same varicosity, depending on the site of release from the active zone of 0.25 μm^2 extent.

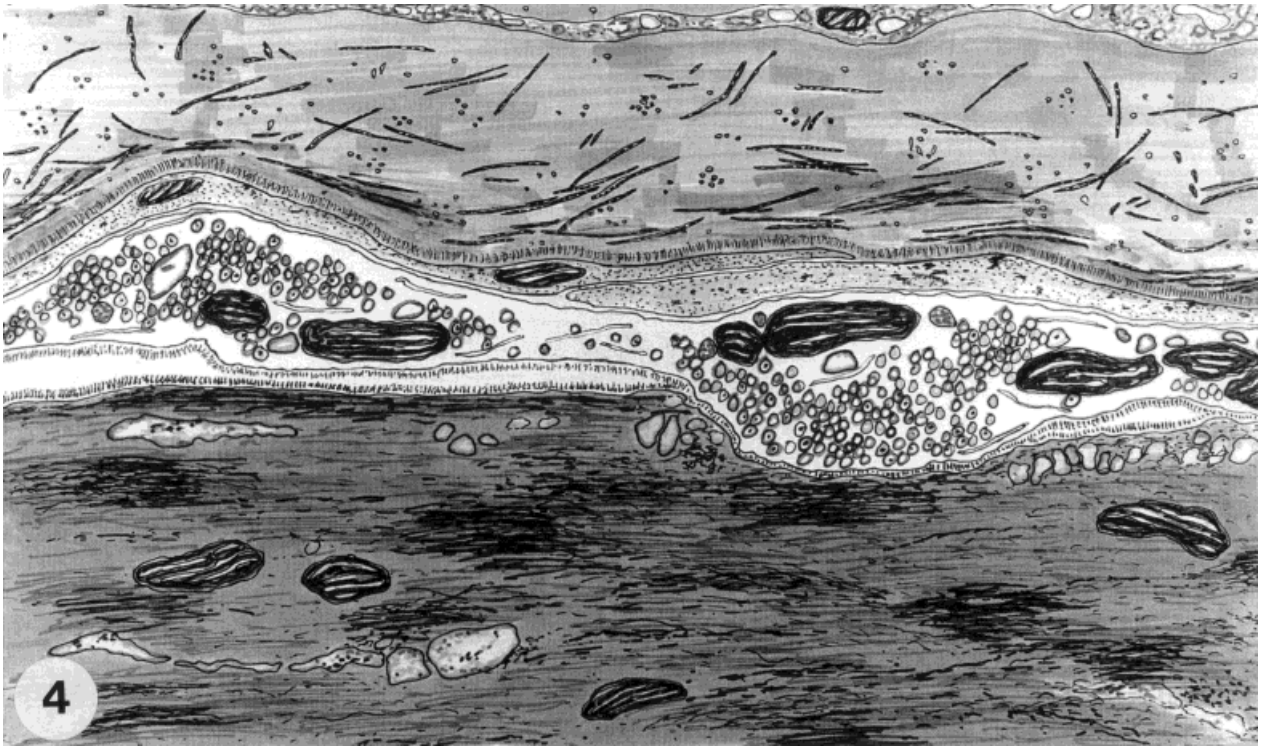

Fig. 4. Diagram of the relationship between a single varicose axon in a visceral smooth muscle and smooth muscle cells. The drawing is for a terminal axon on the surface of the mouse vas deferens. One varicosity comes into close apposition with a smooth muscle cell, such that there is only one layer of basal lamina seperating the axolemma and the smooth muscle cell membrane. In this region of the varicosity, there is a preferential accumulation of synaptic vesicles. However, there are no morphological signs of an active zone in the varicosity axolemma or of a postjunctional specialization. The other varicosity also has an accumulation of vesicles, but in this section it does not come into close apposition with a smooth muscle cell. A very thin layer of Schwann cell membrane separates this terminal axon from the serosa. Diagram by G. Bennett (unpublished observation).

CURRENT FLOW IN THE SMOOTH MUSCLE SYNCYTIUM DURING TRANSMISSION FROM SYMPATHETIC VARICOSITIES

In order to interpret the voltages recorded during junctional transmission, it is necessary to determine how current flows in the electrical syncytium of smooth muscle during transmission. For this purpose we have used bidomain theory. The bidomain analysis of the electrical syncytium is a multidimensional cable analysis that in one dimension reduces to the usual cable analysis with both intracellular and extracellular spaces or domains, giving the bidomain (Eisenberg et al., 1979; Muler and Markin, 1977; Peskoff, 1979; Tung, 1979). In the continuum bidomain analysis the interiors of many interconnected cells are treated as a single continuum of known resistivity, with the interstitial space treated as a second continuum of known resistivity, and both occupying the same overall volume and coupled to each other by the resistance and capacitance of the cell membranes (Tung, 1979). Analytical solutions for the bidomain analysis have been obtained (Gesolowitz and Miller, 1983) and checked using the discrete element analysis (Roth, 1992). The bidomain syncytium analysis has been applied extensively to cardiac muscle over the past few years (for a review see Henriquez, 1993). The anisotropic nature of the cardiac muscle syncytium has also been incorporated into bidomain theory (Bukauskas et al., 1991). The theory has enabled estimates to be made of the way in which the action potential propagates through the syncytium (Henriquez and Plonsey, 1990) as well as estimates of the degree of interaction of electrical activity in adjoining bundles (Plonsey et al., 1988).

We have recently developed a discrete bidomain analysis of the smooth muscle syncytium (Bennett et al., 1993b). In addition we have also begun an analysis of the spread of current and voltage in a three-dimensional bidomain continuum following current injection at a point (Henery et al., 1997). The potential generated in the smooth muscle of the vas deferens on release of a quantum of transmitter from a varicosity has been analyzed using this three-dimensional bidomain continuum. Current is injected at the origin of the bidomain with the temporal characteristics of the junctional current; the membrane potential, intracellular potential, and extracellular potential as well as the extracellular current is then determined throughout the bidomain at different times (Fig. 6). Thus, a solution has been found for the equations describing the temporal changes in the passive spread of current and potential through a three-dimensional bidomain following injection of current at a point. The effect of changing the anisotropy ratios of the intracellular and extracellular conductivities in each of the three dimensions on the spread of current and potential has also been determined. It is shown that the time course of the mem-

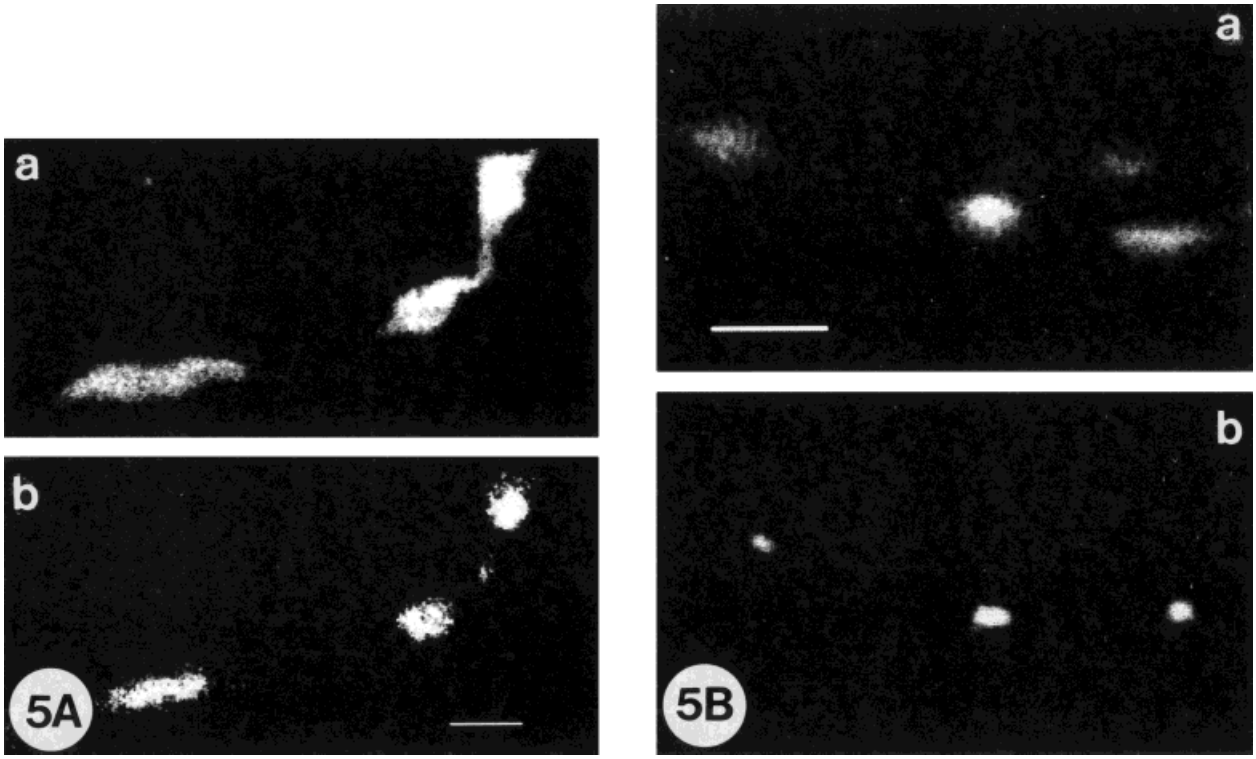

Fig. 5. **A:** Comparison of the size of the varicosity with the size of the area of labelled vesicles. (a) shows a varicose terminal axon filled with orthogradely transported rhodamine-dextran. (b) shows the extent of SV2Ab labelling (FITC-conjugated secondary antibody), which indicates the vesicle distribution in the same terminal axon as that in (a). Calibration bar = 2 µm. **B:** Comparison of the size of the area of labelled vesicles with the area of syntaxin labelling. (a) shows the extent of SV2Ab labelling in a terminal axon. (b) shows the distribution of the syntaxin antibody labelling in the same terminal axon. Calibration bar = 2 µm. Reproduced from Brain et al., 1997, with permission of the publisher.

brane potential changes recorded at any point in the syncytium on the release of a quantum closely follows the time course of the conductance changes produced by the quantum for a wide variety of bidomain properties (Fig. 7). This analysis establishes that the kinetics of transmitter receptor interaction can be studied using the spontaneous excitatory junction potential.

DISTRIBUTION OF RECEPTORS AT SYMPATHETIC VARICOSITIES

The transmitter released from sympathetic varicosities in the vas deferens that is responsible for the electrical signs of transmission is ATP acting on purinergic receptors (Sneddon and Burnstock, 1984; Sneddon and Westfall, 1984). Purinergic receptors involved in this transmission are ATP-gated channels (termed P2x); seven of the P2x receptors are now isolated and expressed (Collo et al., 1996; North, 1996). There are seven known subunits, each encoded by a different gene, and each consisting of two transmembrane domains, a large extracellular loop, as well as intracellular N- and C-termini (Surprenant et al., 1996). All of these proteins are about 36 to 48% identical (Collo et al., 1996). The $P2x_1$ receptor was originally cloned from a complementary DNA that encoded this receptor in the rat vas deferens (Valera et al., 1994), whilst the $P2x_2$ receptor was cloned from rat phaeochromocytoma (PC12) cells (Brake et al., 1994). The permeability of these two receptor types is the same for monovalent cations but the $P2x_1$ receptor has about twice the permeability to calcium ions of the $P2x_2$ receptor (Evans et al., 1996). Two of these purinergic receptors ($P2x_1$ and $P2x_2$) are found in the vas deferens, with immunohistochemistry localizing the $P2x_1$ receptors to smooth muscle cells and the $P2x_2$ receptors to nerve terminals (Vulchanova et al., 1996). $P2x_1$ receptors are found in nerve fibres and terminals of sensory neurons in the dorsal horn but not on nerve fibres in the vas deferens, whereas $P2x_2$ receptors are also found in sensory neurons as well as in the nerve terminals of the vas deferens (Lewis et al., 1995; Vulchanova et al., 1996).

We have developed antibodies against different domains of $P2x_1$ receptors and localized these with respect to the synaptic vesicles in single varicosities using antibodies against the vesicle-associated proteoglycan SV2 (Hansen et al., 1997). This has enabled the distribution of postjunctional purinergic receptors to be determined at the level of individual sympathetic varicosities. High density clusters of $P2x_1$ receptors, about 1 µm in diameter, were found in register with many varicosities, as well as on occasions in regions removed from varicosities (Fig. 8); furthermore, some varicosities did not possess such receptor clusters. The question arises as to the function of such varicosites. One possibility is that although they might not be effective in purinergic transmission, they are in noradrenergic transmission, as there is cotransmission at these junctions (Sneddon and Burnstock, 1984; Sneddon and

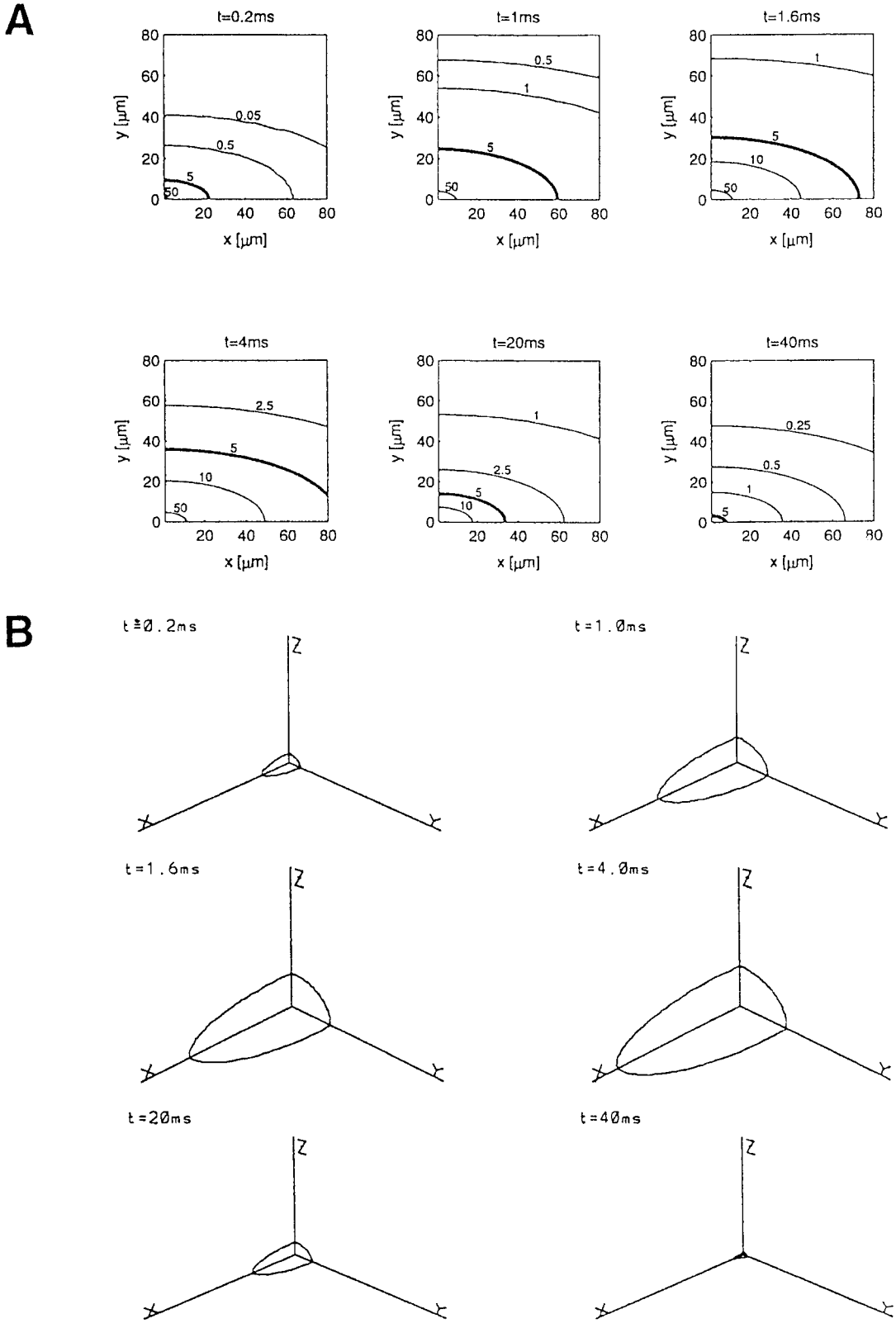

Fig. 6. Calculated membrane isopotential contours (mV) in the smooth muscle bidomain following the release of a quantum of transmitter at six different times for the case of equal anisotropy ratios. The quantal current occurs at the origin with the time course and amplitude given in figure 1 (**A**) in Henery et al. (1997). Contour lines in the x-y plane for the different times indicated after the release of the quantum. **B:** Changes in a single contour plane (that for 5 mV) in the three-dimensional bidomain at different times after the release of the quantum (from Fig. 2 in Henery et al., 1997). Reproduced from Henery et al., 1997, with permission of the publisher.

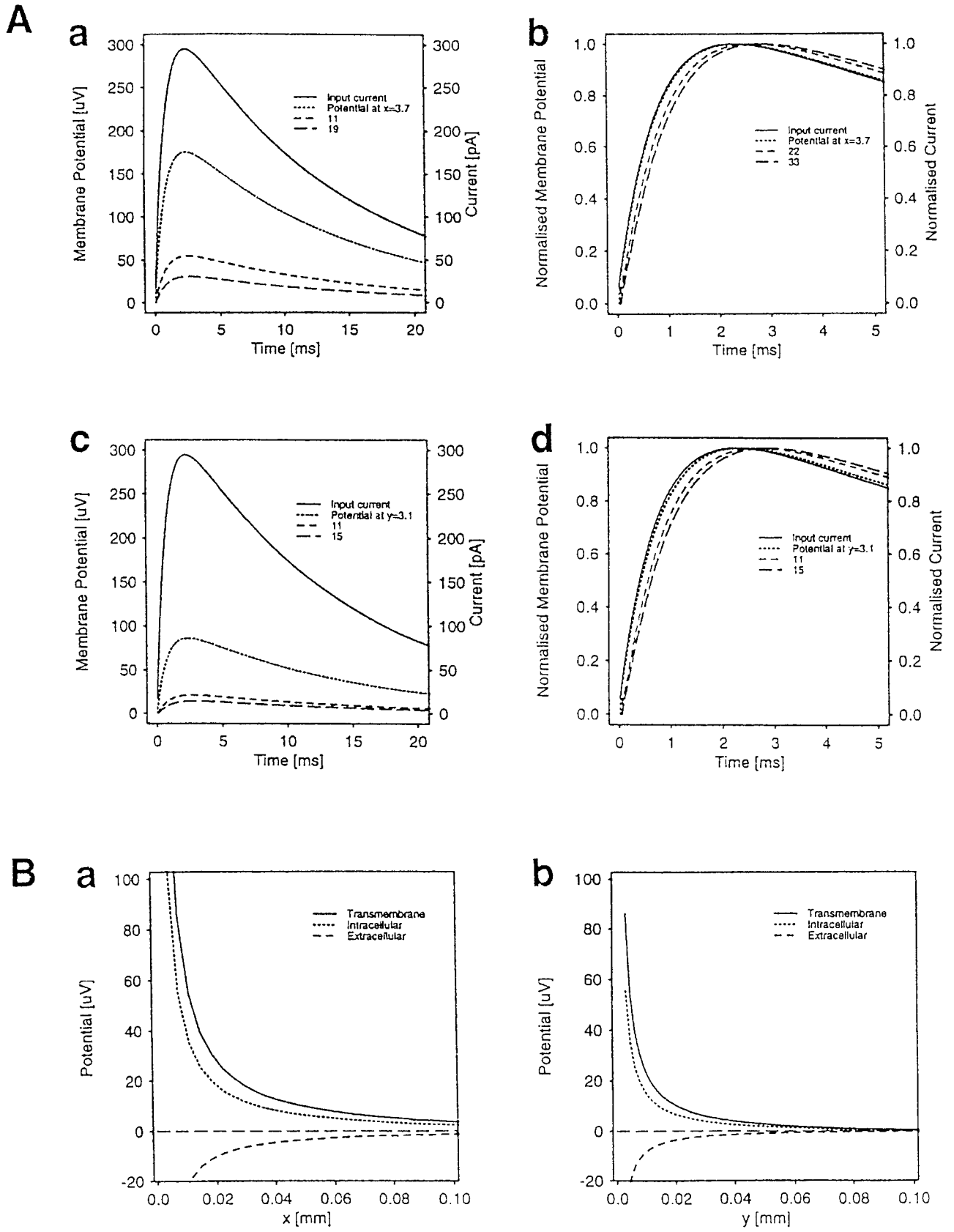

Fig. 7. **A:** Time course of the quantal current at the origin and time course of the membrane potentials at the indicated distances (micrometers) from the origin for the case of equal anisotrophy ratios. (a) and (c) show potentials along the x-axis and y-axis, respectively, while (b) and (d) show normalized potentials on a shorter time scale. **B:** Calculated membrane potential, intracellular potential, and extracellular potential in the x,y directions (z is equivalent to y) in the bidomain at the time of the peak of the quantal current at the origin. (a) and (b) are for the case of equal anisotropy ratios. Reproduced from Henery et al., 1997, with permission of the publisher.

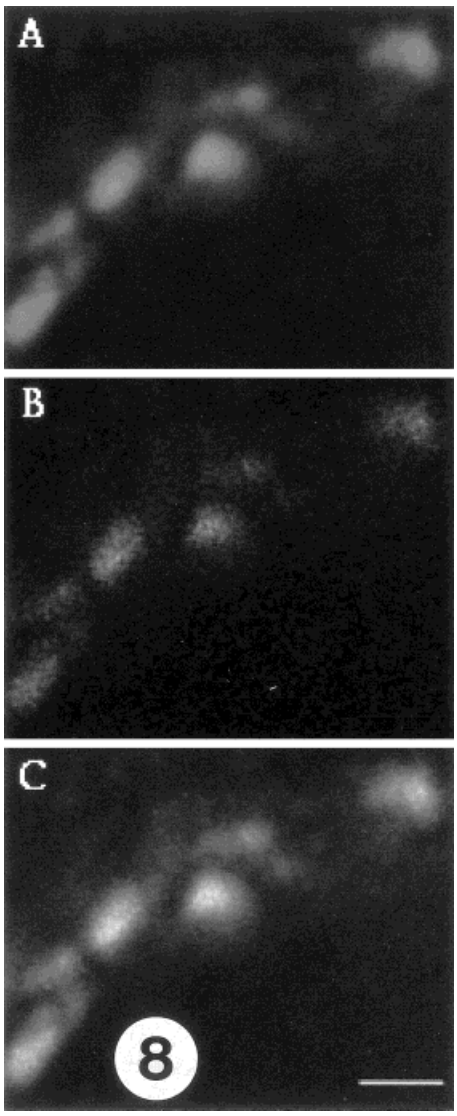

Fig. 8. Immunohistochemical localization of P2x1 purinergic receptors and sympathetic varicosities in smooth muscle of the mouse vas deferens. **A:** Varicosities identified with antibodies to the vesicle associated proteoglycan SV2. **B:** Distribution of high density P2x1 receptor patches in the same section as in A. **C:** Overlap of A and B. Note that all the receptor patches possess an overlying varicosity. Calibration is 2 μm. From Hansen et al., Balcar, Barden and Bennett (unpublished observations).

Westfall, 1984). The distribution of the alpha 1 adrenoceptors on smooth muscle cells that mediate this transmission has not been established; however, it is known that catecholamines can diffuse many microns from a source to affect receptors that require only a single binding to be activated (Hille, 1992); varicosities that do not possess $P2x_1$ receptor clusters may contribute to this noradrenergic transmission.

The question arises concerning the function of the small $P2x_1$ receptor clusters ($\ll$1 μm) found several microns away from any SV2 labelled varicosities. It seems unlikely that varicosities fail to label with SV2 as this proteoglycan is found on all synaptic vesicles throughout the nervous system. The existence of receptor clusters without overlying presynaptic membranes has also been observed at the only other site in the peripheral nervous system for which there are receptor labels for an ionotropic receptor, namely that for acetylcholine receptors on autonomic ganglion cells (Horch and Sargent, 1995). In this case, it has been shown that there are two classes of clusters, one that is large with a high density of receptors and occurring in relatively low frequency with another that is smaller with a lower density of receptors and occurring at a relatiely high frequency (Horch and Sargent, 1996). About 20% of the large clusters are not colocalized at synaptic boutons, although they tend to be in the vicinity of these; none of the small clusters are colocalized at boutons (Horch and Sargent, 1996). These authors suggest that the small clusters and the large extrasynaptic clusters may represent intermediates in the metabolism of large synaptic clusters. Monte Carlo simulations of the affects of ACh released from a bouton onto a colocalized ACh receptor patch with an immediately adjacent extrasynaptic receptor patch show that the released ACh can activate some of these extrasynaptic receptors, making substantial contributions to the amplitude-frequency histogram of synaptic potentials recorded in the ganglion cell (see fig. 5D in Bennett and Brain, 1997). Both the nicotinic ACh receptors in ganglia and the $P2x_1$ receptors on smooth muscle cells require double bindings of agonist to be activated. This places severe constraints on the possibility that extrasynaptic receptors several microns away from the site of transmitter release can be activated (Bennett et al., 1995). The idea of Horch and Sargent (1996) concerning the role of extrasynaptic ACh receptor clusters, namely that they are intermediates in the metabolism of the synaptic clusters, may also be applicable for the extrajunctional $P2x_1$ receptor clusters.

The $P2x_1$ receptors are not only localized in receptor clusters, but are also found in low density over all the smooth muscle cells in the vas deferens. Experiments using [^{3}H]alpha beta-methylene ATP to label P2x receptors in smooth muscles have already shown that all the cells of a smooth muscle are likely to possess P2x receptors. Autoradiography has shown binding of the radioligand to cells throughout smooth muscles (Balcar et al., 1995; Bo and Burnstock, 1993). The low density $P2x_1$ receptors over the surface of all the smooth muscle cells detected by autoradiography may be the small extrajunctional receptor clusters mentioned above. If diffusion of ATP to these clusters occurs from varicosities then they may be the prime mediators of junctional transmission, even given the caveats about such transmission mentioned above. Bennett and Gibson (1995) have argued that it is only the rising phase of the junctional currents during sympathetic neuromuscular transmission that are occassionaly affected by the release of a quantum of ATP from a varicosity forming a close apposition with a smooth muscle cell; most of the junctional current may arise from activation of the bulk of the $P2x_1$ receptors present in the large number of small $P2x_1$ receptor clusters found over the entire surface of the muscle cells.

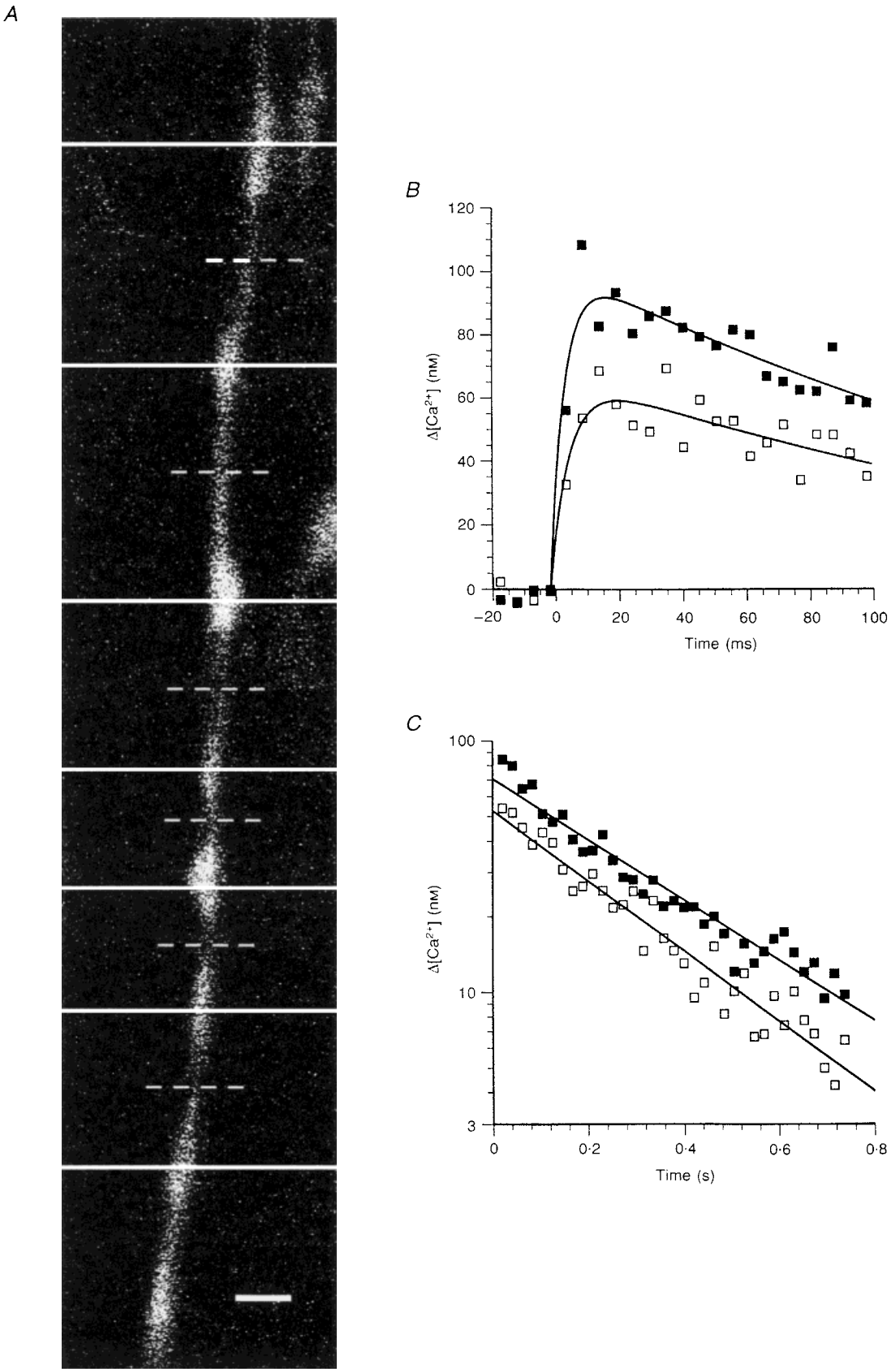

Fig. 9. Changes in $[Ca^{2+}]_v$ in contiguous varicosities and intervaricosity regions after an impulse. **A:** Composite image of the chain of varicosities from which line scans were taken. Each frame in the composite was captured 10–15 seconds before the relevant line scan in order to record the location of the region being sampled. The horizontal continuous lines indicate the line sampled from when recording from a varicosity. The dashed lines indicate the locations of line scans through intervaricose regions. The scale bar = 2 µm. Some refocusing was required between frames in order to place the varicosity of interest in the plane of focus. **B:** Average change in $[Ca^{2+}]_v$ measured with line scans through 7 contiguous varicosities (filled squares) and the 6 intervening intervaricose regions (open squares), from A. Shown is the period from 20 ms before the impulse to 100 ms after the impulse. The fitted curve is the sum of two exponentials. **C:** Same data set as in B, over a longer time period of the declining phase on log-linear co-ordinates. Reproduced from Brain and Bennett, 1997, with permission of the publisher.

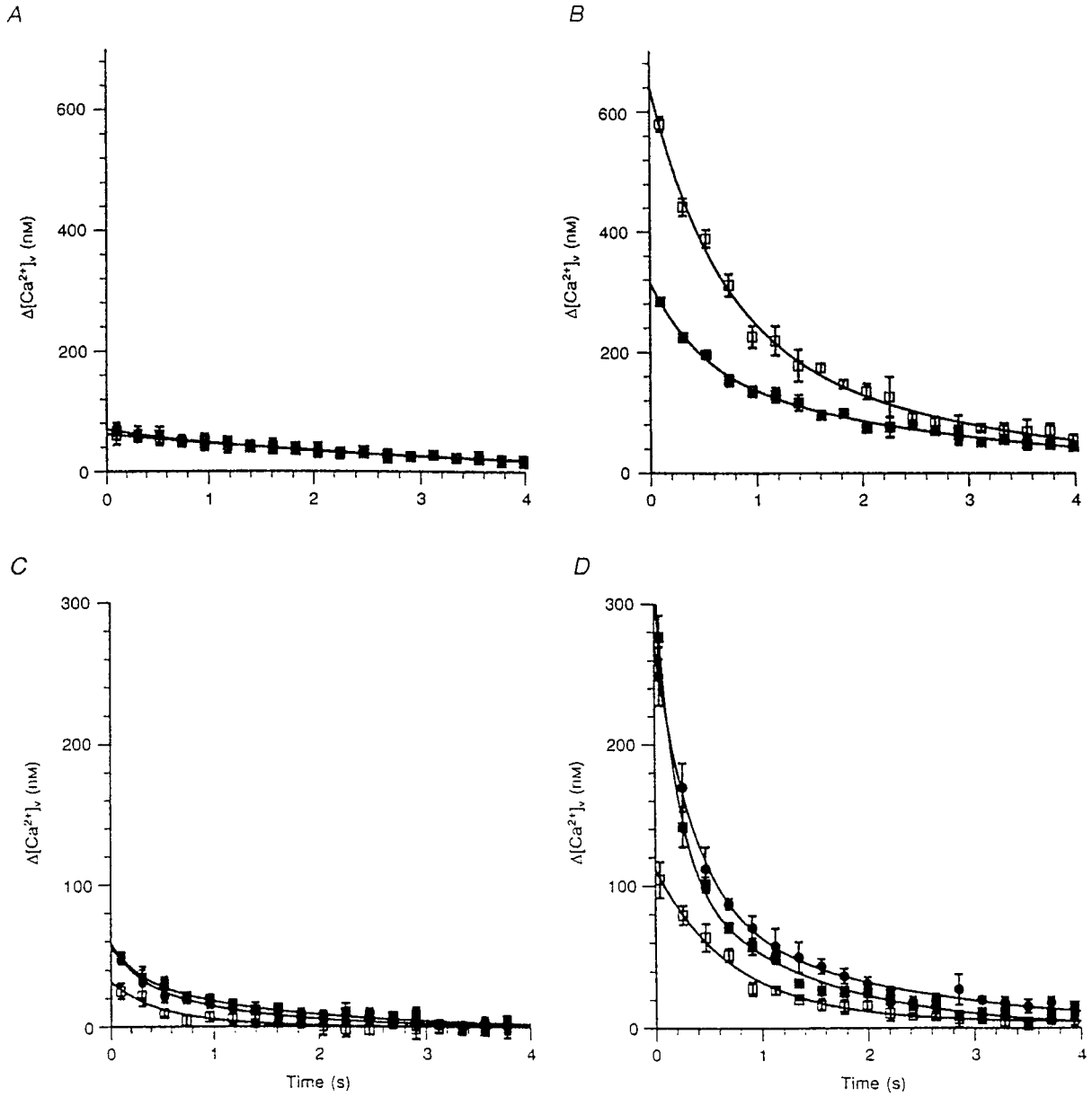

Fig. 10. The effect of alpha 2 adrenoceptor agonists and antagonists on $[Ca^{2+}]_v$. **A:** Results for the $[Ca^{2+}]_v$ in a single varicosity following single impulses before the application of Yohimbine (filled squares) and in the presence of Yohimbine (10 mM; open squares). **B:** Results for $[Ca^{2+}]_v$ following stimulation with a 5-impulse train before the application of (filled squares) and in the presence of Yohimbine (10 mM; open squares). **C:** Results for the $[Ca^{2+}]_v$ in the same varicosity following a single impulse before the application of (filled squares) and in the presence of clonidine (1 mM; open squares). When Yohimbine was applied to the bath solution and the response to single impulses was recorded (filled circles), this effect was reversed. **D:** $[Ca^{2+}]_v$ in a varicosity following a 5-impulse train at 5 Hz before the application of (filled squares) and in the presence of clonidine (1 mM; open squares). Once more, this effect could be reversed with Yohimbine (10 mM; open squares). Each point in B and D is the mean of 6 different stimulations for this varicosity, taken 2 minutes apart, corrected by the average of 2 control recordings. Each point in A and C is the mean of 3 different stimulations for this varicosity, taken 2 minutes apart, corrected by the average of 2 control recordings. Reproduced from Brain and Bennett, 1997, with permission of the publisher.

CALCIUM TRANSIENTS IN SINGLE SYMPATHETIC VARICOSITIES AND TRANSMITTER SECRETION

The study of calcium transients in individual sympathetic varicosities following an impulse, and their modulation by classical alpha 2 adrenoceptors on the varicosity membrane, has recently been initiated (Brain and Bennett, 1997). Calcium indicators are loaded into the nerve terminals by the technique of orthograde transport of dextran coupled indicators placed on the cut sympathetic axons, using the same technique mentioned above in relation to the loading of rhodamine into varicosities. Confocal microscope using line scans allows for a temporal resolution of a few ms in catching the changes in indicator fluorescence following an impulse. Figure 9A shows such line scans through a

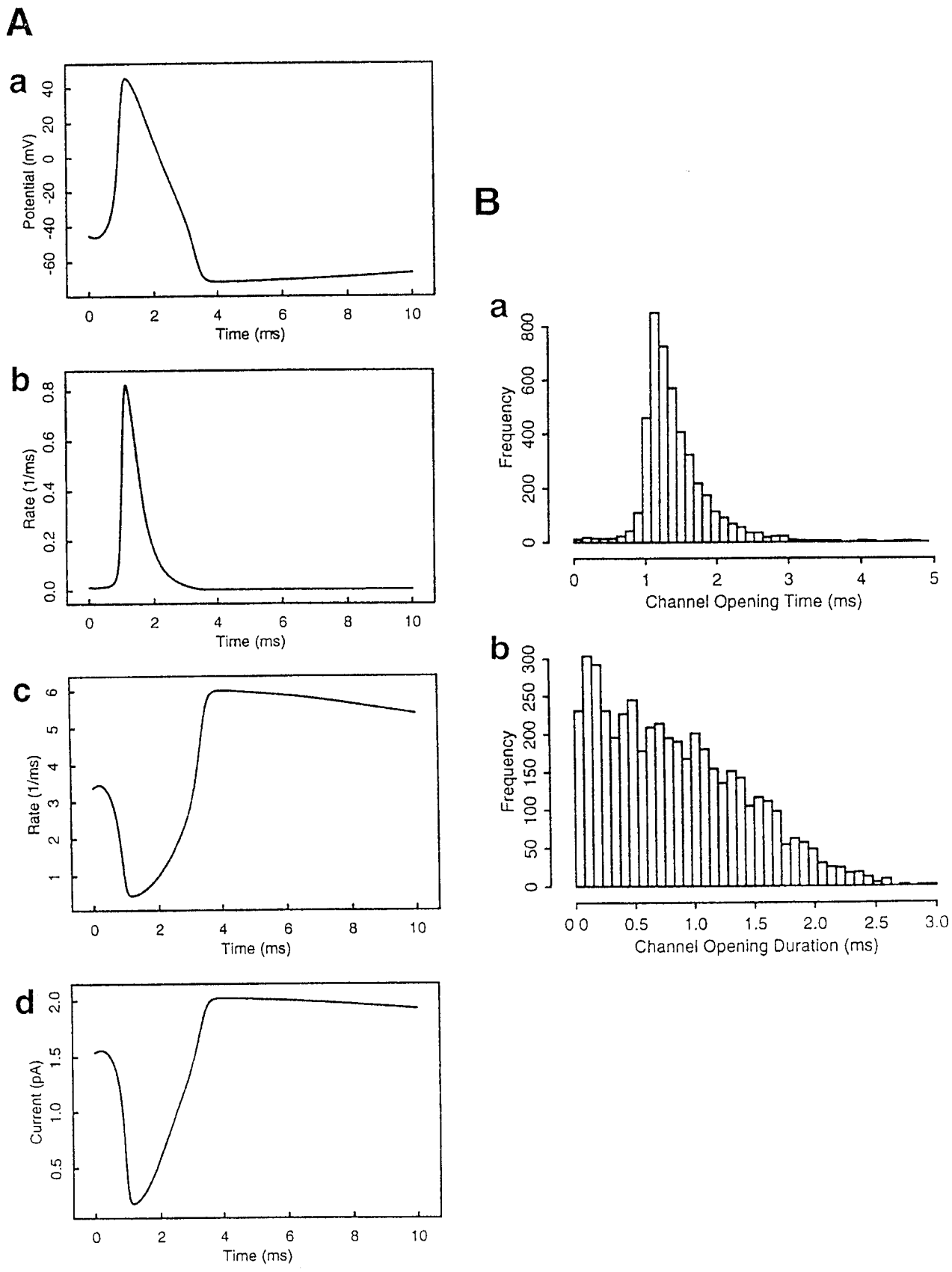

Fig. 11. **A:** Behaviour of a calcium channel during an impulse. **a:** The time course of the impulse according to the solution of the Hodgkin-Huxley equations. **b:** The time dependence of the forward rate constant k_1 during the Hodgkin-Huxley impulse, according to Eq. 3. **c:** The time dependence of the reverse rate constant k_{-1} during the Hodgkin-Huxley impulse, according to Eq. 4. **d:** The time dependence of the magnitude of the ionic current, i(t), through a single calcium channel during the Hodgkin-Huxley impulse, given that the channel is open throughout the impulse, according to Eq. 8. (see Bennett et al., 1997, for the equations mentioned here). **B:** Histograms of the times at which a calcium channel opens (**a**) and the duration of the open time (**b**) for a channel under an impulse. A total of 4,638 openings were obtained for a run of 10,000 impulses. Reproduced from Bennett et al., 1997, with permission of the publisher.

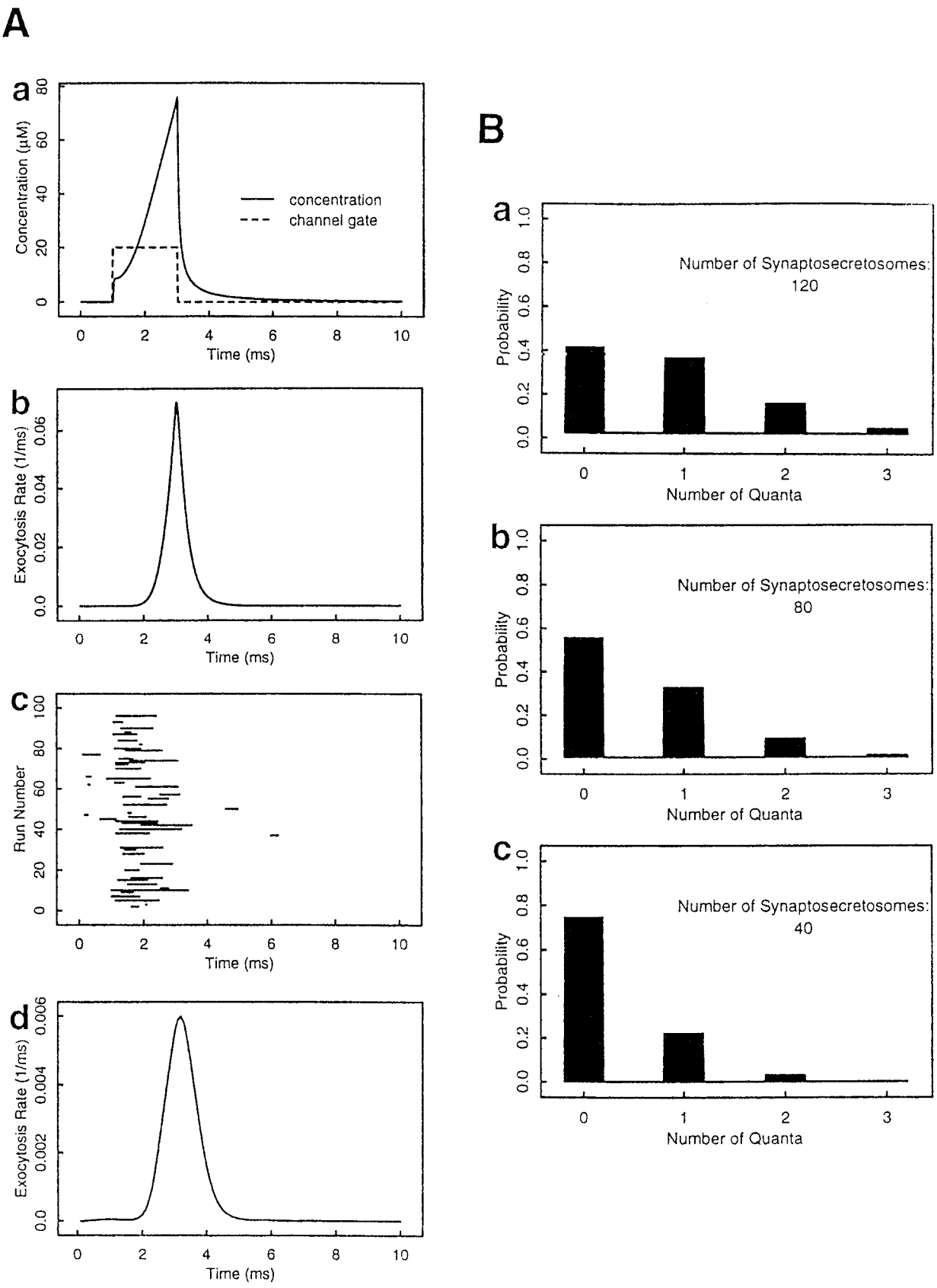
A
a
Concentration (μM)
concentration
channel gate
Time (ms)
b
Exocytosis Rate (1/ms)
Time (ms)
c
Run Number
Time (ms)
d
Exocytosis Rate (1/ms)
Time (ms)
B
a
Probability
Number of Synaptosecretosomes:
120
Number of Quanta
b
Probability
Number of Synaptosecretosomes:
80
Number of Quanta
c
Probability
Number of Synaptosecretosomes:
40
Number of Quanta

Fig. 12.

series of varicosities (continuous horizontal lines) and intervaricosities (broken horizontal lines) of a single string of varicosities in the vas deferens. Comparison between the calcium transients in the varicosities and intervaricosities following an impulse shows that the time course of increase in calcium concentration in the intervaricosites is about the same as that in the varicosities, to within about 3 ms (Fig. 9B), suggesting that the calcium increase in the intervaricosities is due to a direct flux of calcium across their membranes rather than to the diffusion of calcium from the varicosities. The peak calcium concentration reached in the intervaricosities at this time is comparable to that in the varicosities, with the subsequent sequestration of the calcium occurring over the same time courses (Fig. 9C). Given the much smaller volume of the intervaricosities compared with that of the varicosities, the observations indicate that the density of voltage-dependent calcium channels of the N-type, which pass the bulk of the calcium influx (Brain and Bennett, 1997), is much lower for the intervaricosities than for the varicosities.

This technique of directly measuring the calcium influx into single varicosities following an impulse allows for tests of whether different drugs that act to modulate transmitter release do so by modulating calcium influx into varicosities. For instance, the question of whether activation of prejunctional alpha 2 adrenoceptors leads to a decrease in the release of transmitter from sympathetic nerve terminals can now be directly ascertained. Figure 10 shows that while yohimbine does not affect the calcium influx following a single impulse (Fig. 10A), it markedly increases the calcium influx into a varicosity following a short train of 5 impulses at 5 Hz, without changing the rates of calcium sequestration (Fig. 10B). It is known that noradrenaline released by a single impulse does not inhibit transmitter release by that impulse, but it does that of subsequent impulses, so these observations on calcium transients show that activation of alpha 2 adrenoceptors by noradrenaline inhibits calcium influx into the varicosities. In order to test this another way, the alpha 2 adrenoceptor agonist clonidine was used: in this case the calcium influx into a single varicosity due to a single impulse was significantly depressed (Fig. 10C) as was that due to 5 impulses at 5 Hz (Fig. 10D). The study of calcium influxes into single varicosities opens up a new approach to the pharmacology of presynaptic mechanisms in sympathetic nerve terminals.

The calcium influx into a sympathetic varicosity following a nerve impulse is primarily through N-type calcium channels that are likely to be in close proximity with the vesicle associated proteins that act as the calcium sensor for triggering the exocytosis of a vesicle. This sensor is very likely to be synaptotagmin (Sudhof, 1995). This protein contains two copies of an internal repeat that is homologous to the regulatory region of protein kinase C. The protein altogether contains five domains: a single transmembrane at the N-terminus that spans the membrane of the synaptic vesicle; a sequence separating the transmembrane region from the two repeats (C2a and C2b) that are homologous to the protein kinase C; the two repeats homologous to protein kinase C with C2a closest to this transmembrane region; and a carboxyl terminal sequence following these two repeats (Perin et al., 1991). Synaptotagmin may be anchored at its C-terminal end to the pre-synaptic membrane bound protein syntaxin (Bennett et al., 1993a). As antibodies to syntaxin immunoprecipitate N-type calcium channels (Bennett et al., 1993a), and there is known to be a direct interaction between the cytoplasmic domains of both syntaxin and the N-type channel (Sheng et al., 1994), it is likely that a tight structural association exists between synaptotagmin, syntaxin, and the N-type calcium channel. This combination has been termed the "synaptosecretosome" by O'Connor et al. (1993), and is abbreviated here to "secretosome."

At present the use of low affinity calcium indicators together with confocal microscopy only allows calcium transients to be detected in a minimum volume of about $600 \times 600 \times 600$ nm. This is substantially greater than the volume occupied by the transient high calcium level reached during the opening of an N-type calcium channel in the secretosome, which is likely to be of the order of $50 \times 50 \times 50$ nm, as the distance between synaptotagmin and the channel is between 25 and 50 nm (Stanley, 1993). At the present time then one must resort to Monte Carlo modelling of the calcium transient within the secretosome and the triggering of exocytosis by synaptotagmin on the arrival of an nerve impulse in order to obtain some insights into the calcium-triggered secretory process in a sympathetic varicosity. To this end, we have provided a stochastic description of the opening of an N-type calcium channel under a Hodgkin-Huxley impulse, the subsequent diffusion of calcium ions from the open channel to synaptotagmin, and the stochastic interaction of these ions with the four binding sites on the molecule that, when occupied, trigger exocytosis through changes in synaptotagmin (Bennett et al., 1997). Figure 11A(d) shows the calcium current throught the channel under the action potential in Figure 11A(a), given that the channel is open throughout the duration of the action potential: the changes in the forward [Fig. 11A(b)] and reverse rate constants

Fig. 12. **A:** Probability of exocytosis for a vesicle opening under an impulse. The vesicle, with its calcium-sensitive vesicle-associated proteins is located 20 nm from a calcium channel (together these comprise the synaptosecretosome). **a:** The change in calcium concentration at the calcium sensor (solid line), obtained by evaluating Eq. 1 for the particular case of a channel opening at 1.0 ms and closing at 3.0 ms, as depicted by the broken curve. **b:** The rate of exocytosis (dP_{ex}/dt) of the vesicle for the case illustrated in a, using the standard single-affinity rate constants (see table 2 in Bennett et al., 1997). **c:** The times of opening and closing of a calcium channel during different impulses that resulted in 50 openings during the time interval 0–10 ms; the length of each line gives the open time for that run. (These are part of a stimulation involving 1,000 impulses in which 434 openings occurred, the remainder giving no opening during the interval 0–10 ms). **d:** The corresponding rate of exocytosis when the channel opens stochastically; the graph shows the average of 1,000 impulses, which resulted in 434 channel openings. **B(a):** The probability p_k of a single Hodgkin-Huxley impulse leading to the exocytosis of k vesicles from n independent synaptosecretosomes when the probability of each exocytosis is p. The value P = 0.00731 is calculated using the standard single-affinity rate constants, and the probabilities are found from the binomial distribution as $p_k = b(k; n,p)$. **b:** Bouton case, for which the assumption of a two-dimensional regular-grid array of synaptosecretosomes leads to the estimate n = 80. **c:** Motor nerve terminal case, for which the assumption of a one-dimensional regular spacing of synaptosecretosomes leads to the estimate n = 40. Reproduced from Bennett et al., 1997, with permission of the publisher. The equation and table referred to are in that paper.

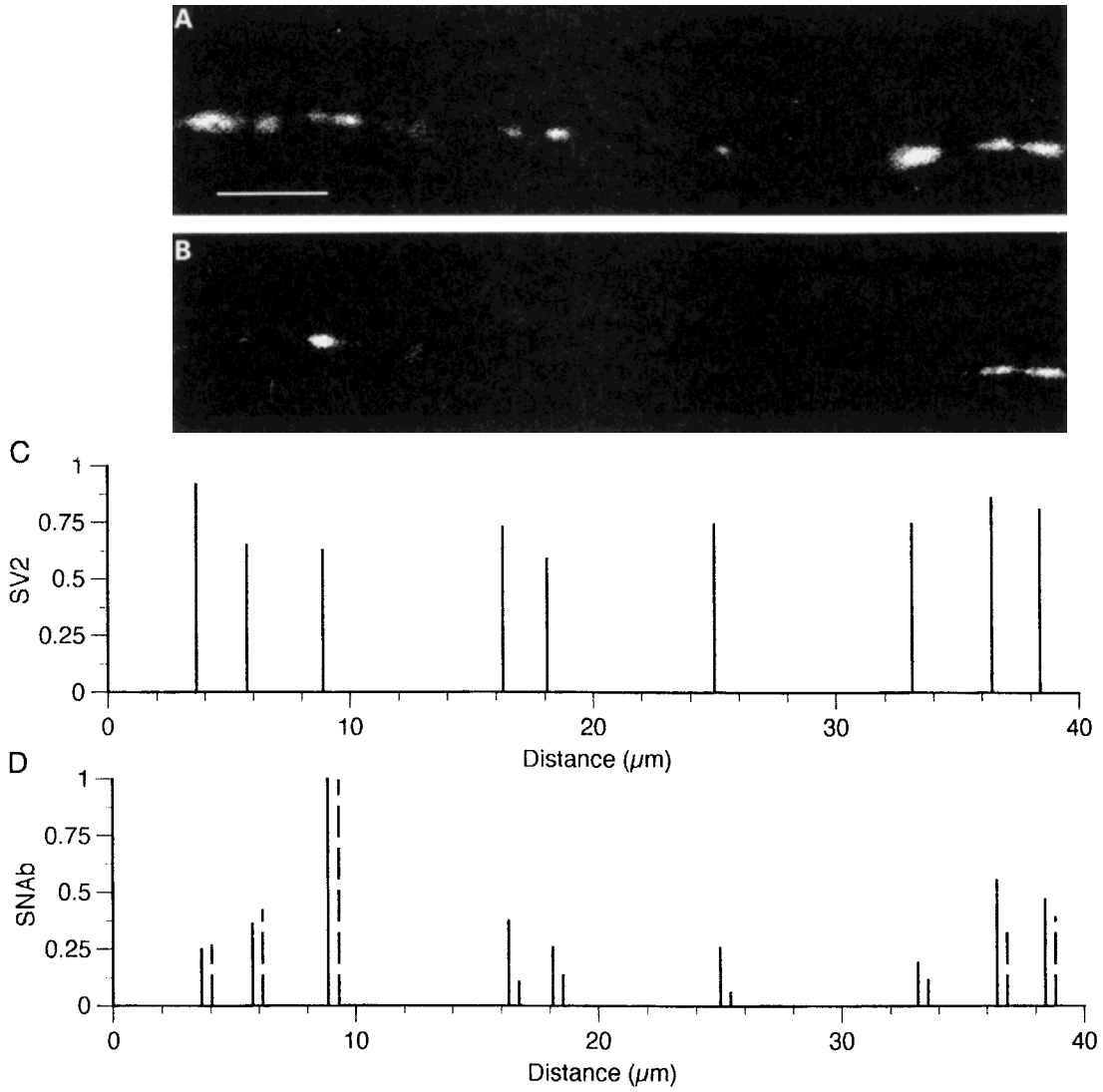

Fig. 13. Expression of SV2Ab and SNAb in varicosities of a sympathetic terminal axon during stimulation. **A:** Varicose sympathetic terminal axon identified with the SV2Ab (FITC-conjugated secondary antibody). **B:** Same terminal axon labelled with the RNAb in the presence of 80 mM potassium for 30 minutes before subsequent fixation (rhodamine-conjugated secondary antibody). **C:** Quantification of the extent of SV2Ab labelling along the length of the set of varicosities shown in A and B; the ordinate is the relative average intensity of fluorescence. **D:** Quantification of the extent of rhodamine fluorescence (SNAb) along the length of the set of varicosities shown in A and B; the ordinate is relative fluorescence for the solid vertical lines, and relative average intensity of fluorescence multiplied by the area of the fluorescence in the varicosity for the broker vertical lines. The distance scale in A and B is not quite the same as that in C and D because the distance in the former pair is measured between the midpoints of the varicosities, rather than recording the horizontal distance. Calibration bar in A (for A,B) = 5 μm. Reproduced from Brain et al., 1997, with permission of the publisher.

[Fig. 11A(c)] of the channel with a change in potential together with the changes in driving force for calcium ions during the impulse give rise to a calcium current that is greatest during the after-hyperpolarization of the action potential. However, the opening and closing of channels are non-homogeneous Poisson processes. Solving for the open time and closed time density function allows estimates to be made over several thousand impulses of the distribution of times at which a channel opens under an impulse and the duration of the open time (Fig. 11B). It is found that a channel opens for at least some time on about 50% of occasions on the arrival of the impulse and that the average open time is 0.8 ms with most openings occurring between 1 and 2 ms after the beginning of the impulse (Fig. 11B). It is interesting in this regard that Sakmann and his colleagues have recently shown that about 70% of the channels in the calyciform terminal in the nucleus of Held open on arrival of a nerve impulse (Sakmann, personal communication). If the concentration of calcium ions at synaptotagmin in the secretosome is next ascertained by solution of the diffusion equations for calcium diffusing from the open channel to the calcium sensor [Fig. 12A(a)], then calculation of the stochastic interaction of these ions with the sensor protein gives the rate of exocytosis [Fig. 12A(b)]. Consideration of the stochastic opening of the calcium channel in the secretosome over many impulses gives the pattern of opening and closing times for channels shown in Figure 12A(c) allowing determination of the rate of exocytosis in

Figure 12A(d), which is the average exocytosis over 1,000 impulses.

The purpose of these calculations is to provide estimates for the expected probability of secretion from a varicosity due to the calcium influx through an N-type calcium channel associated with a secretosome. This can be carried out, under the assumption that the secretosomes act independently, by simply applying the binomial law to each varicosity that possess n secretosomes, given that the probability for exocytosis from a secretosome, p, has been determined by the stochastic analysis briefly described above. Figure 12B shows the probability of a single Hodgkin-Huxley impulse giving rise to the exocytosis of k vesicles, when the number of secretosomes in each varicosity is 120 (a), 80 (b), and 40 (c). It will be noted that even when there are as few as 40 secretosomes in a varicosity there are still occasions in which two quanta are released on the arrival of an impulse [Fig. 12B(c)]. These calculations show that the average quantal content of the release from a varicosity with only 40 secretosomes is 0.2, whereas that for a varicosity with 120 secretosomes is 0.6. Such variations in the quantal release from single varicosities along the length of sympathetic nerve terminals have been observed using loose-patch electrode recording from individual varicosities (Lavidis and Bennett, 1993).

It is frequently observed during loose-patch recording from sympathetic varicosities on the vas deferens that the probability of secretion from the varicosity is zero. In the absence of spontaneous quantal secretions from these varicosities, the possibility exists that they may not possess a $P2x_1$ receptor patch beneath them, a situation that has been observed in studies of the distribution of $P2x_1$ receptor clusters and varicosities labelled with SV2 antibody. In order to avoid such difficulties, another measure of the probability of secretion from varicosities has been developed that is not dependent on the interaction of quanta with the postjunctional receptor patch to give an electrical sign of transmitter release. This involves taking advantage of the fact, mentioned in relation to the structure of the secretosome, that the N-terminus of synaptotagmin resides on the inside face of the synaptic vesicle. Thus, when a vesicle undergoes exocytosis and exposes its inside to the medium outside the nerve terminal, the N-terminus is at least momentarily exposed to the outside medium. We have made peptides identical to the N-terminus of synaptotagmin and developed antibodies to these, which, when fluorescently tagged, label the N-terminus of synaptotagmin. Exposure of the nerve terminal to these antibodies during stimulation then permanently tags those vesicles that have undergone exocytosis. Experiments of this kind on strings of varicosities in the vas deferens show that there is considerable non-uniformity in the probability of secretion from the varicosities (Fig. 13; Brain et al., 1997). If the varicosities are identified by their vesicular complement with antibodies to SV2 (Fig. 13A), then only relatively few of them are intensely labelled with antibodies to the N-terminus on stimulation (Fig. 13B). Quantitative evaluation of this result shows that there is a fairly even intensity of fluorescence labelled antibody to SV2 in the different varicosities of a string (Fig. 13C) whereas the intensity of fluorescence labelled antibody to the N-terminus varies greatly between varicosities, by at least fourfold (Fig. 13D). These observations show that there is considerable non-uniformity of quantal release between even adjacent varicosities, confirming the electrophysiological analysis using loose-patch electrodes over varicosities.

CONCLUSION

In this short essay, the most recent observations in this laboratory on the mechanism of transmission at single sympathetic varicosities in the vas deferens have been described. The active zone of individual sympathetic varicosities, delineated by a high concentration of syntaxin, occupies an area on the prejunctional membrane of about 0.2 μm^2; this gives a junctional gap between the prejunctional active zone and postjunctional membranes that varies between about 50 and 100 nm. The postjunctional membrane beneath the varicosity can possess a patch about 1 μm^2 of purinergic $P2x_1$ receptors in high density, although this is not always the case; more diffuse $P2x_1$ receptor distributions are also found on the muscle cells unrelated to varicosities.

A nerve impulse gives rise to a transient increase in calcium concentration in every varicosity, primarily due to the opening of N-type calcium channels, as well as to a smaller increase in the intervaricose regions. ATP released from the varicosities is modulated by the concomitant release of noradrenaline that acts on the varicosities through alpha 2 adrenoceptors to decrease the influx of calcium ions that accompanies the nerve impulse. Solution of the equations for the stochastic opening of the N-type calcium channel under an action potential, with diffusion of calcium ions to the calcium sensor synaptotagmin in the secretosome, and subsequent stochastic activation of synaptotagmin leading to exocytosis of a vesicle in the secretosome, allowed for determination of the probability of secretion at individual varicosities. These probabilities varied between different varicosities depending on the number of secretosomes in the varicosity. The observations on the probability of secretion of quanta from adjacent varicosities made with loose-patch electrodes were similar to those obtained from the calculations if the number of secretosomes per varicosity varied between 40 and 120. Such variations in the probability for secretion from adjacent varicosities were confirmed using labelling of the N-terminus of synaptotagmin as an indicator of quantal transmission. The next task is to give a quantitative account of the calcium flux into a secretosome on arrival of the nerve impulse, as well as of the number of secretosomes that each varicosity possesses and of the factors that control this variation in the number of secretosomes per active zone that appear to be the likely determinant of the probability of secretion.

REFERENCES

Balcar, V.J., Li, Y., Killinger, S., and Bennett, M.R. (1995) Autoradiography of P2x ATP receptors in the rat brain. Br. J. Pharmacol., 115:302–306.

Bennett, M.R. (1996a) Autonomic neuromuscular transmission at a varicosity. Prog. Neurobiol., 50:505–532.

Bennett, M.R. (1996b) Neuromuscular transmission at an active zone: The secretosome hypothesis. J. Neurocytol., 25:869–891.

Bennett, M.R., and Brain, K. (1997) Autonomic synaptic transmission at single boutons and calyces. J. Neurocytol., 26:577–603.

Bennett, M.R., and Gibson, W.G. (1995) On the contribution of quantal secretion from close-contact and loose-contact varicosities to the synaptic potentials in the vas deferens. Phil. Trans. R. Soc. Lond. Ser. B., 347:187–204.

Bennett, M.K., Garcia-Arravas, J.E., Elferink, L.A., Peterson, K., Fleming, A.M., Hazuka, C.D., and Scheller, R.H. (1993a) The syntaxin family of vesicular transport receptors. Cell, 74:863–873.

Bennett, M.R., Gibson, W.G., and Poznanski, R.R. (1993b) Extracellular current flow and potential during quantal transmission from varicosities in a smooth muscle syncytium. Phil. Trans. R. Soc. Long. Ser. B., Biol. Sci., 342:89–99.

Bennett, M.R., Farnell, L., Gibson, W.G., and Karunanithi, S. (1995) Quantal transmission at purinergic junctions: Stochastic interaction between ATP and its receptors. Biophys. J., 68:925–935.

Bennett, M.R., Gibson, W.G., and Robinson, J. (1997) Probabilistic secretion of quanta and the synaptosecretosome hypothesis: Evoked release at active zones of varicosities, boutons and endplates. Biophys. J., 73:1815–1829.

Bo, X., and Burnstock, G. (1993) Heterogeneous distribution of [^{3}H]alpha, beta-methylene ATP binding sites in blood vessels. J. Vasc. Res., 30:87–101.

Boudier, J.A., Charvin, N., Boudier, J.L., Fathallah, M., Tagaya, M., Takahashi, M., and Seagar, M.J. (1996) Distribution of components of the SNARE complex in relation to transmitter release sites at the frog neuromuscular junction. Eur. J. Neurosci., 8:545–552.

Brain, K.L., and Bennett, M.R. (1997) Calcium in sympathetic varicosities of mouse vas deferens during facilitation, augmentation and autoinhibition. J. Physiol., 502:521–536.

Brain, K.L., Cottee, L.J., and Bennett, M.R. (1997) Varicosities of single sympathetic nerve terminals possess syntaxin zones and different synaptotagmin N-terminus labelling following stimulation. J. Neurocytol., 26:491–500.

Brake, A.J., Wagenbach, M.J., and Julius, D. (1994) New structural motif for ligand-gated ion channels defined by an ionotropic ATP receptor. Nature, 371:519–523.

Bukauskas, F., Bytantas, A., Gutman, A., and Veteikis, R. (1991) Simulation of passive electrical properties in two- and three-dimensional anisotropic syncytial media. In: Intracellular Communication. F. Bukauskas, ed. Manchester University Press, Manchester, NY.

Collo, G., North, R.A., Kawashima, E., Merlo-Pich, E., Neidhart, S., Surprenant, A., and Buell, G. (1996) Cloning of P2X5 and P2X6 receptors and the distribution and properties of an extended family of ATP-gated ion channels. J. Neurosci., 16:2495–2507.

Cottee, L.J., Lavidis, N.A., and Bennett, M.R. (1996) Spatial relationships between sympathetic varicosities and smooth muscle cells in the longitudinal layer of the mouse vas deferens. J. Neurocytol., 25:413–425.

Dale, H.H. (1934) Chemical transmission of the effects of nerve impulses. Br. Med. J., 1:835–841.

del Castillo, J., and Katz, B. (1954) Quantal components of the endplate potential. J. Physiol., 124:560–573.

Eisenenberg, R.S., Barcilon, V., and Mathias, R.T. (1979) Electrical properties of spherical syncytia. Biophy. J., 25:151–180.

Elliott, T.R. (1904) The action of adrenaline. J. Physiol., 32:401–467.

Evans, R.J., Lewis, C., Virginio, C., Lundstrom, K., Buell, G., Surprenant, A., and North, R.A. (1996) Ionic permeability of, and divalent cation effects on two ATP-gated cation channels (P2X receptors) expressed in mammalian cells. J. Physiol. 497:413–422.

Fatt, P., and Katz, B. (1951) An analysis of the end-plate potential recorded with an intracellular electrode. J. Physiol., 115:320–370.

Geselowitz, D.B., and Miller, W.T. (1983) A bidomain model for anisotropic cardiac muscle. Ann. Biomed. Eng., 11:191–206.

Hansen, M.A., Barden, J.A., Balcar, V.J., Keay, K.A., and Bennett, M.R. (1997) Structural motif and characteristics of the extracellular domain of P2X receptors. Biochem. Biophys. Res. Commun., 236:670–675.

Henery, R., Gibson, W.G., and Bennett, M.R. (1997) Quantal currents and potential in the three-dimensional anisotropic bidomain model of smooth muscle. Bull Math. Biol., 59:1047–1075.

Henriquez, C.S. (1993) Simulating the electrical behaviour of cardiac tissue using the bidomain model. Crit. Rev. Biomed. Eng., 21:1–77.

Henriquez, C.S., and Plonsey, R. (1990) Simulation of propagation along a cylindrical bundle of cardiac tissue. I: Mathematical formulation. IEEE Trans. Biomed. Eng., 37:850–860.

Hillarp, N.A. (1946) Structure of the synapse and the peripheral innervation apparatus of the autonomic nervous system. Acta. Anat., (Suppl. IV):1–153.

Hille, B. (1992) G protein-coupled mechanisms and nervous signalling. Neuron, 9:187–195.

Horch, H.L., and Sargent, P.G. (1995) Perisynaptic surface distribution of multiple classes of nicotinic acetylcholine receptors on neurones in the chicken ciliary ganglion. J. Neurosci., 15:7778–7795.

Horch, H.L., and Sargent, P.B. (1996) Effects of denervation on acetylcholine receptor clusters on frog cardiac ganglion neurones as revealed by quantitative laser scanning confocal microscopy. J. Neurosci., 16:1720–1729.

Katz, B. (1996) Neural transmitter release: from quantal secretion to exocytosis and beyond. The Fenn Lecture. J. Neurocytol., 25:677–686.

Katz, B., and Miledi, R. (1973) The effect of alpha-bungarotoxin on acetylcholine receptors. Br. J. Pharmacol. 49:138–139.

Langley, J.N. (1898) On the union of cranial autonomic (visceral) fibres with the nerve cells of the superior cervical ganglion. J. Physiol., XXIII:240–270.

Langley, J.N. (1901) Observations on the physiological action of extracts of the supra-renal bodies. J. Physiol., 27:237–256.

Langley, J.N. (1906) On nerve endings and on special excitable substances in cells. Proc. R. Soc. Lond. B., 78:170–194.

Lavidis, N.A., and Bennett, M.R. (1993) Probabilistic secretion of quanta from successive sets of visualized varicosities along single sympathetic nerve terminals. J. Autonom. Nerv. Syst., 43:41–50.

Lewis, C., Neidhart, S., Holy, C., North, R.A., Buell, G., and Suprenant, A. (1995) Coexpression of P2X2 and P2X3 receptor subunits can account for ATP-gated currents in sensory neurones Nature, 377:385–386.

Macleod, G.T., Lavidis, N.A., and Bennett, M.R. (1994) Calcium dependence of quantal secretion from visualized sympathetic nerve varicosities on the mouse vas deferens. J. Physiol., 480:61–70.

Merrillees, N.C.R. (1968) The nervous environment of individual smooth muscle cells of the guinea pig vas deferens. J. Cell Biol., 37:794–817.

Muler, A.L., and Markin, V.S. (1977) Elektricheskie svoistva anizotropnykh nervnomyshechnykh sintsitiev. I. Raspredelenie elektrotonicheskogo potentsiala. Biofizika, 22:307–312.

North, R.A. (1996) P2x receptors: A third major class of ligand-gated ion channels. Ciba Found. Symp., 198:91–105.

O'Connor, V.M., Shamotienko, O., Grishin, E., and Betz, H. (1993) On the structure of the "synaptosecretosome." Evidence for a neurexin/synaptotagmin/syntaxin/Ca^{2+} channel complex. FEBS Lett., 326: 255–260.

Perin, M.S., Johnston, P.A., Ozcelik, T., Jahr, R., Francke, U., and Sudhof, T.C. (1991) Structural and functional conservation of synaptotagmin (p65) in Drosophila and neurones. J. Biol. Chem., 266:615–622.

Peskoff, A. (1979) Electric potential in three-dimensional electrically syncytial tissues. Bull. Math. Biol., 41:163–181.

Plonsey, R., Henriquez, C., and Trayanova, N. (1988) Extracellular (volume conductor) effect on adjoining cardiac muscle electrophysiology. Med. Biol. Eng. Comp., 26:126–129.

Richardson, K.C. (1962) Fine structure of autonomic nerve endings in smooth muscle of the rat vas deferens. J. Anat., 96:427–442.

Roth, B.J. (1992) How the anisotropy of the intracellular and extracellular conductivities influences stimulation of cardiac muscle. J. Math. Biol., 30:633–646.

Sheng, Z.H., Rettig, J., Takahashi, M., and Catterall, W.A. (1994) Identification of a syntaxin-binding site on N-type calcium channels. Neuron, 13:1303–1313.

Sneddon, P., and Burnstock, G. (1984) Inhibition of excitatory junction potentials in guinea-pig vas deferens by alpha, beta-methylene-ATP: further evidence for ATP and noradrenaline as cotransmitters. Eur. J. Pharmacol., 100:85–90.

Sneddon, P., and Westfall, D.P. (1984) Pharmacological evidence that adenosine triphosphate and noradrenaline are co-transmitters in the guinea-pig vas deferens. J. Physiol., 347:561–580.

Stanley, E.F. (1993) Single calcium channels and acetylcholine release at a presynaptic nerve terminal. Neuron, 11:1007–1011.

Sudhof, T.C. (1995) The synaptic vesicle cycle: a cascade of protein-protein interactions. Nature, 375:645–653.

Surprenant, A., Rassendren, F., Kawashima, E., North, R.A., and Buell, G. (1996) The cytolytic P2z receptor for extracellular ATP identified as a P2x receptor (P2x7). Science, 272:735–738.

Thomson, P.C., Lavidis, N.A., Robinsin, J., and Bennett, M.R. (1995) Probablistic secretion of quanta at somatic motor-nerve terminals: the fusion-pore model, quantal detection and autoinhibition. Phil. Trans. Roy. Soc. Lond. B, 349:197–214.

Tung, L. (1979) Three dimensional cable theory: A bidomain model. Biophys. J., 25:214A.

Valera, S., Hussy, N., Evans, R.J., Adami, N., North, R.A., Surprenant, A., and Buell G. (1994) A new class of ligand-gated ion channel defined by P2x receptor for extracellular ATP. Nature, 371:516–519.

Vulchanova, L., Arvidsson, U., Riedl, M., Wang, J., Buell, G., Surprenant, A., North, R.A., and Elde, R. (1996) Differential distribution of two ATP-gated channels (P2x receptors) determined by immunocytochemistry. Proc. Natl. Acad. Sci. U.S.A., 93:8063–8067.